Inorganic Chemistry

Article

pubs.acs.org/IC

Nonchromophoric Halide Ligand Variation in Polyazine-Bridged Ru(II),Rh(III) Bimetallic Supramolecules Offering New Insight into Photocatalytic Hydrogen Production from Water

Hannah Mallalieu Rogers,* Travis A. White, Brittany N. Stone, Shamindri M. Arachchige, and Karen J. Brewer†

Department of Chemistry, Virginia Tech, Blacksburg, Virginia 24061, United States

ABSTRACT: The new bimetallic complex $[(Ph_2phen)_2Ru(dpp)RhBr_2(Ph_2phen)](PF_6)_3$ (**1**) (Ph_2phen = 4,7-diphenyl-1,10-phenanthroline; dpp = 2,3-bis(2-pyridyl)pyrazine) was synthesized and characterized to compare with the Cl^- analogue $[(Ph_2phen)_2Ru(dpp)RhCl_2(Ph_2phen)](PF_6)_3$ (**2**) in an effort to better understand the role of halide coordination at the Rh metal center in solar H_2 production schemes. Electrochemical properties of complex **1** display a reversible $Ru^{II/III}$ oxidation, and cathodic scans indicate multiple electrochemical mechanisms exist to reduce Rh(III) by two electrons to Rh(I) followed by a quasi-reversible $dpp^{0/-}$ ligand reduction. The weaker σ-donating ability of Br^- vs Cl^- impacts the cathodic electrochemistry and provides insight into photocatalytic function by these bimetallic supramolecules. Complexes **1** and **2** exhibit identical light-absorbing properties with UV absorption dominated by intraligand (IL) $\pi \rightarrow \pi^*$ transitions and visible absorption by metal-to-ligand charge transfer (MLCT) transitions to include a lowest energy $Ru(d\pi) \rightarrow dpp(\pi^*)$ ^{1}MLCT transition (λ^{abs} = 514 nm; ε = 16 000 M^{-1} cm^{-1}). The relatively short-lived, weakly emissive $Ru(d\pi) \rightarrow dpp(\pi^*)$ ^{3}MLCT excited state (τ = 46 ns) for both bimetallic complexes is attributed to intramolecular electron transfer from the ^{3}MLCT excited state to populate a low-energy $Ru(d\pi) \rightarrow Rh(d\sigma^*)$ triplet metal-to-metal charge transfer (^{3}MMCT) excited state that allows photoinitiated electron collection. Complex **1** outperforms the related Cl^- bimetallic analogue **2** as a H_2 photocatalyst despite identical light-absorbing and excited-state properties. Additional H_2 experiments with added halide suggest ion pairing plays a role in catalyst deactivation and provides new insight into observed differences in H_2 production upon halide variation in Ru(II),Rh(III) supramolecular architectures.

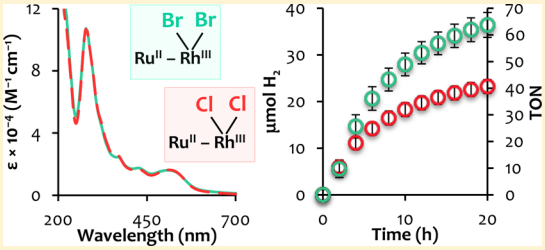

INTRODUCTION

Hydrogen gas is a highly desired alternative to carbon-based fuels and can be formed via water splitting through solar energy conversion schemes.[1−3] To achieve artificial photosynthetic processes such as water splitting, the field of inorganic supramolecular chemistry shows promise with the design of molecules capable of performing complex tasks.[4,5] Supramolecular complexes, as described by Balzani, are intricate molecules comprised of subunits that each contribute to the overall task performed by the complex.[6] Photochemical molecular devices (PMDs) are a subclass of supramolecular complexes that carry out demanding photoinitiated processes made possible by judicious choice of molecular subunits. Transition metal complexes that absorb light and participate in excited-state reactions are ideal PMD candidates.[7−9] A prototypical light absorber, $[Ru(bpy)_3]^{2+}$ (bpy = 2,2′-bipyridine) is extensively studied in solar energy conversion schemes due to desirable redox activity and stability, intense UV and visible light absorption, a long-lived charge transfer excited state, and rapid oxidative or reductive quenching capabilities to afford electron transfer.[10−13] Substituting one or more polypyridyl terminal ligands (TL) (e.g., bpy in $[Ru(bpy)_3]^{2+}$) with a polypyridyl bridging ligand (BL) (e.g., dpp; bpm = 2,2′-bipyrimidine) allows the construction of supramolecular architectures assembled through coordinate covalent linkage of molecular subunits.[14−18]

Supramolecular complexes that collect two or more reducing equivalents via photochemical processes are termed photoinitiated electron collectors (PECs). Complexes exist that function as PECs but are not catalytically active due to collection of reducing equivalents at a noncatalytic site.[19−23] The first use of a PEC to photocatalytically reduce H_2O to H_2 was reported for $[\{(bpy)_2Ru(dpp)\}_2RhCl_2]^{5+}$, possessing Ru light absorber subunits linked through dpp BLs to a Rh center.[24] The trimetallic photocatalyst functions through successive visible light excitations, reductive quenching by a sacrificial electron donor, and electron collection at a reactive metal permitted by low-lying $Rh(d\sigma^*)$-based acceptor orbitals to produce H_2 by reduction of H_2O.[24]

Component modification via terminal ligand and/or halide variation was studied in architectures of the form $[\{(TL)_2Ru(dpp)\}_2RhX_2]^{5+}$ (where TL = bpy, phen (1,10-phenanthroline), or Ph_2phen; X = Cl^- or Br^-).[25−27] Within this motif, the TL = Ph_2phen and X = Br^- trimetallic complex is the highest performing H_2 photocatalyst.[27] Ph_2phen is a superior TL due to

Received: January 16, 2015
Published: March 17, 2015

DOI: 10.1021/acs.inorgchem.5b00116
Inorg. Chem. 2015, 54, 3545−3551

increased visible light absorption, increased lifetime of the ^{3}MLCT excited state, and enhanced driving force for H_2 production relative to TL = bpy and phen analogues. The weaker σ-donating ability of X = Br^- vs Cl^- is thought to contribute to more efficient generation of the Rh(I) active catalyst following photoinitiated electron collection. However, after one turnover of the catalyst, the same Ru(II),Rh(I),Ru(II) photocatalyst predominates regardless of halide identity, thus not identifying the disparity in long-term catalyst stability when the halide coordinated to Rh is varied. For each set of TLs in the previously studied Ru(II),Rh(III),Ru(II) trimetallic series, the light-absorbing properties do not change upon halide variation, while the X = Cl^- analogues have larger quantum yields of emission (Φ^{em}) and longer excited-state lifetimes (τ). Smaller Φ^{em} and shorter τ in the X = Br^- analogues suggest more efficient population of a low-lying metal-to-metal charge transfer (^{3}MMCT) excited state, an important parameter for H_2O reduction by these photocatalysts that leads to more efficient H_2 photocatalysis.[25−27]

When the number of light-absorbing units is decreased from two to one within Ru(II),Rh(III) supramolecules, a bimetallic motif results. A balance of proper steric and electronic components is required to achieve catalysis as demonstrated with component modification in the Ru(II),Rh(III) bimetallic architecture. The complex $[(phen)_2Ru(dpp)RhCl_2(bpy)]^{3+}$ undergoes PEC but does not serve as a photocatalyst for H_2 production due to the lack of steric bulk at Rh, permitting Rh(I)−Rh(I) dimerization which prevents species coordination necessary to further the catalytic cycle.[28] Complex $[(Ph_2phen)_2Ru(dpp)RhCl_2(Ph_2phen)]^{3+}$ (**2**) containing a bulky, weakly electron-donating Ph_2phen TL on Rh serves as a photocatalyst for H_2 production, while $[(bpy)_2Ru(dpp)RhCl_2(^tBu_2bpy)]^{3+}$ with a bulky, more strongly electron-donating $^tBu_2bpy$ TL on Rh does not produce H_2 under identical conditions.[29] The disparity in photocatalytic activity is attributed to the bulky TLs electronically modulating the lowest unoccupied molecular orbital (LUMO) which is BL-based with TL = $^tBu_2bpy$ and Rh-based when TL = Ph_2phen, giving evidence for the necessity of a lowest lying Rh-based acceptor orbital to achieve H_2 photocatalysis.[30] The Ru(II),Rh(I) bimetallic complexes $[(TL)_2Ru(dpp)Rh^I(COD)]$ (TL = bpy or Me_2bpy (4,4′-dimethyl-2,2′-bipyridine); COD = 1,5-cyclooctadiene) serve as H_2 photocatalysts with steric protection about the Rh(I) center provided by the COD ligand,[31] further demonstrating the importance of steric effects to produce H_2O reduction photocatalysts.

With knowledge of the relative orbital energetics and steric requirements to achieve H_2 production photocatalysts, complex **1** was characterized and studied to better understand the role of the nonchromophoric halide ligand in H_2 photocatalysis. The synthesis, photophysical characterization, and H_2 production studies are reported herein for this Ru(II),Rh(III) bimetallic with comparison to the Cl^- analogue **2**. The excited-state properties will be explored to determine the impact of halide ligand variation on Φ^{em} and τ values for the bimetallic system. On the basis of halide variation studies within related Ru(II),Rh(III),Ru(II) trimetallic architectures,[25−27] complex **1** is predicted to outperform **2** as a photocatalyst for H_2 production, and insight on the influence of halide identity on catalytic function with regard to ion pairing will be discussed.

EXPERIMENTAL SECTION

Materials. All chemicals were used as received unless otherwise noted. The reagents $RuCl_3·3H_2O$, $RhCl_3·3H_2O$, $RhBr_3·3H_2O$, trifluoromethanesulfonic acid (CF_3SO_3H), 4,7-diphenyl-1,10-phenanthroline (Ph_2phen), and tetra-*n*-butylammonium chloride (Bu_4NCl) were purchased from Alfa Aesar. 2,3-Bis(2-pyridyl)pyrazine (dpp), tetra-*n*-butylammonium bromide (Bu_4NBr), *N*,*N*-dimethylaniline (DMA), and Sephadex LH-20 were purchased from Sigma-Aldrich Corp. Ammonium hexafluorophosphate (NH_4PF_6) was purchased from Strem Chemicals, Inc. Tetra-*n*-butylammonium hexafluorophosphate (Bu_4NPF_6) was purchased from Fluka. Spectral-grade acetonitrile and *N*,*N*-dimethylformamide (DMF) were purchased from Burdick and Jackson. Ethanol (100%) was purchased from Decon Laboratories, Inc. Toluene, diethyl ether, methanol, and 80−200 mesh adsorption alumina were purchased from Fischer Scientific. Complexes $[(Ph_2phen)_2RuCl_2]$ (**1a**),[32] $[(Ph_2phen)_2Ru(dpp)](PF_6)_2$ (**1b**),[17,33] and $[(Ph_2phen)_2Ru(dpp)RhCl_2(Ph_2phen)](PF_6)_3$ (**2**)[29] were prepared as previously reported.

Synthesis. Complex $[(Ph_2phen)RhBr_3(DMF)]$ (**1c**) was synthesized similar to a previously reported method.[34] The starting materials $RhBr_3·3H_2O$ (0.10 g, 0.26 mmol) and Ph_2phen (0.09 g, 0.26 mmol) were combined with 2 mL of DMF and heated in a 60 °C oil bath for 2 h. Upon cooling to RT, an orange solid was precipitated in diethyl ether, dried under vacuum, and washed with water and diethyl ether (0.15 g, 0.21 mmol, yield = 77%). ESI-MS: $[M + NH_4^+]$, m/z = 766.86. The chloride Rh monometallic, $[(Ph_2phen)RhCl_3(DMF)]$, was synthesized using the above method using $RhCl_3·3H_2O$ (0.10 g, 0.38 mmol) and Ph_2phen (0.13 g, 0.38 mmol). Upon synthesis and purification, a yellow solid was collected (0.16 g, 0.26 mmol, yield =70%). ESI-MS: $[M + H^+]$, m/z = 614.00.

Complex $[(Ph_2phen)_2Ru(dpp)RhBr_2(Ph_2phen)](PF_6)_3$ (**1**) was synthesized similar to a previously reported method.[29] Complex **1b** (0.078 g, 0.061 mmol) was reacted with **1c** (0.050 g, 0.067 mmol) in 15 mL of 2:1 (v/v) ethanol/water at reflux for 2 h. Upon cooling to RT, the sample was added dropwise to 30 mL of an aqueous NH_4PF_6 solution to induce precipitation as a PF_6^- salt. A maroon precipitate was collected via vacuum filtration and washed with excess water and diethyl ether. The crude sample was purified using Sephadex LH-20 size-exclusion chromatography with a 2:1 (v/v) ethanol/acetonitrile mobile phase. A maroon band eluted first and was collected, rotary evaporated, dissolved in a minimal amount of acetonitrile, and reprecipitated in diethyl ether. A maroon solid was collected via vacuum filtration and rinsed with excess diethyl ether (0.049 g, 0.024 mmol, yield = 48%). ESI-MS: $[M - 2PF_6^-]^{2+}$, m/z = 870.05.

Mass Spectrometry. Samples were analyzed using electrospray ionization time-of-flight mass spectrometry with an Agilent Technologies 6220 Accurate-Mass TOF LC-MS with a dual ESI (electrospray ionization) source to obtain high-resolution mass spectral data. The solvent used was HPLC-grade acetonitrile.

Electrochemistry. Cyclic voltammograms were obtained using a Bioanalytical Systems (BAS) Epsilon electrochemical analyzer. In a three-electrode, one-compartment cell, 0.1 M Bu_4NPF_6 in spectrophotometric-grade CH_3CN was the supporting electrolyte solution. The working electrode was a platinum disk, and the auxiliary electrode was a platinum wire. The Ag wire pseudoreference electrode was calibrated against the ferrocene/ferrocenium ($FeCp_2/FeCp_2^+$) redox couple as an internal standard (0.46 V vs Ag/AgCl) at the end of each set of scans.[35] Cyclic voltammograms were obtained at a scan rate of 100 mV s^{-1}.

Electronic Absorption Spectroscopy. Electronic absorption spectra were obtained using a Hewlett-Packard 8453 diode array spectrophotometer. Using a sampling interval of 1 nm, measurements were obtained in a wavelength range of 190−1100 nm. Measurements were carried out in a 0.2 or 1 cm path length quartz cuvette (Starna Cells, Inc., Atascadero, CA) in RT spectral-grade acetonitrile. Extinction coefficient measurements were performed in triplicate.

Steady-State and Time-Resolved Emission Spectroscopy. Steady-state emission spectra were measured using a QuantaMaster Model QM-200-45E fluorimeter from Photon Technologies Interna-

DOI: 10.1021/acs.inorgchem.5b00116
Inorg. Chem. 2015, 54, 3545−3551

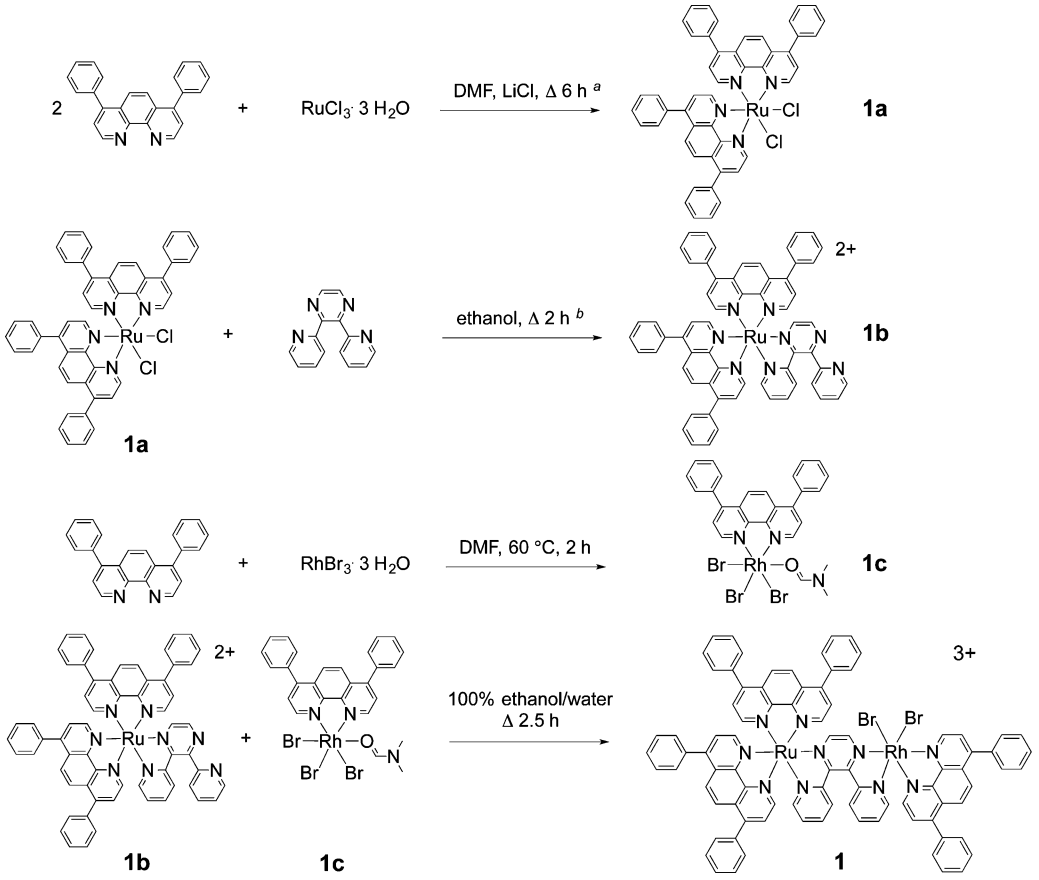

Figure 1. Building block synthetic scheme for the preparation of **1**. [a]Reference 32. [b]Reference 33.

tional, Inc. Spectra were obtained using a 1 cm path length quartz cuvette, and RT measurements were taken in deoxygenated spectral-grade CH_3CN. The excitation source was a water-cooled 150 W xenon arc lamp, and the emission spectra were obtained at a 90° angle with a thermoelectrically cooled Hamamatsu R2658 photomultiplier tube operating in photon counting mode with 0.25 nm resolution. The quantum yields of emission were measured relative to $[Os(bpy)_3]^{2+}$ (Φ^{em} = 4.62 × 10^{-3}).[36] Low-temperature emission spectra were collected in a 4:1 (v/v) ethanol/methanol solution cooled to 77 K using liquid N_2 in a finger Dewar to form the rigid glass matrix. Emission spectra were corrected for PMT response using the manufacturer-supplied correction file.

The excited-state lifetimes were measured using a Photon Technologies International, Inc. PL-2300 nitrogen laser with an attached PL-201 tunable dye laser. The excitation monochromator was set to 540 nm, and emission from the sample was detected at a 90° angle from the excitation source by passing through an emission monochromator set to 780 nm with a Hamamatsu R928 photomultiplier tube operating in direct output mode. The signal was recorded using a LeCroy 9361 oscilloscope, averaging the results of 300 sweeps.

The rate constants for intramolecular electron transfer (k_{et}) for **1** and **2** were found by calculating the rate constants for radiative decay (k_r) and nonradiative decay (k_{nr}) utilizing $[\{(Ph_2phen)_2Ru\}_2(dpp)]^{4+}$, the model bimetallic complex that lacks a ^{3}MMCT excited state.[27,31]

Photolysis Experiments. Experiments carried out to measure H_2 production employing photocatalysts **1** and **2** were performed similar to previously reported methods.[24] Stock catalyst solutions prepared in DMF were combined with water in the photolysis reaction cell that was sealed with a 10 mm airtight septum. The catalyst in the DMF/water mixture was deoxygenated with Ar for approximately 10 min prior to injecting the separately deoxygenated DMA electron donor. The final volume of the photocatalytic solution was 4.5 mL (130 μM photocatalyst, 0.62 M H_2O, 1.5 M DMA, 0.11 mM $[DMAH^+][CF_3SO_3^-]$) with a headspace volume of 16.0 mL. For designated experiments, a total concentration of 260 μM Bu_4NX (Bu_4N = tetrabutylammonium; X = Br^- or Cl^-) in DMF solution was present in the photolysis solution keeping other concentrations consistent with previous experiments. The solution was photolyzed using a 470 nm LED array constructed in our laboratory (LED array light flux = 2.36 ± 0.05 × 10^{19} photons/min).[37] HY-OPTIMA 700 in-line process solid-state H_2 sensors from H_2scan (Valencia, CA) were connected using an airtight septum to the reaction cell to monitor H_2 production in real time. The reported value for H_2 production is an average of three experiments.

RESULTS AND DISCUSSION

Synthesis. Using a building block method, individual molecular components were prepared systematically to produce the target molecule **1** (Figure 1). Complex **1a** was prepared by reacting 2 equiv of the bidentate terminal ligand, Ph_2phen, with $RuCl_3{\cdot}3H_2O$.[32] The highly luminescent $[Ru(Ph_2phen)_3]^{2+}$ impurity was removed using alumina adsorption chromatography. Next, the labile Cl^- ligands were removed under reflux in the presence of a bis-bidentate BL to assemble **1b**.[33] The new Rh(III) monometallic **1c** was prepared in high yield by reacting $RhBr_3{\cdot}3H_2O$ with Ph_2phen in DMF, and purification was achieved by washing with water.[34] The monometallic precursors **1b** and **1c** were reacted in a 2:1 (v/v) ethanol/water solution to produce the new bimetallic complex **1** which was precipitated by metathesis in an aqueous NH_4PF_6 solution.

Compared to related trimetallic complexes of the form $[\{(TL)_2Ru(dpp)\}_2RhX_2]^{5+}$ (TL = terminal ligand; X = Cl^- or Br^-),[25−27] Ru(II),Rh(III) bimetallic complexes discussed herein are more synthetically challenging to prepare because

DOI: 10.1021/acs.inorgchem.5b00116
Inorg. Chem. 2015, 54, 3545−3551

of the need for a Rh(III) precursor containing only one bidentate ligand, Ph_2phen in this system. Rh(III) prefers to form bis-chelated species, as with *cis*-$[(NN)_2RhX_2]^+$ complexes (NN = bidentate polypyridyl ligand; X = Cl^- or Br^-);[38−40] thus, mild conditions were necessary to prepare precursor **1c** for the target bimetallic species. The new complex **1** was characterized using ESI-MS, electrochemical analysis, electronic absorption spectroscopy, and time-resolved and steady-state emission spectroscopy.

Electrochemistry. Complex **1** was analyzed using cyclic voltammetry to provide insight into the frontier orbital energetics and redox-active nature of the supramolecule and related precursors (Figure 2).

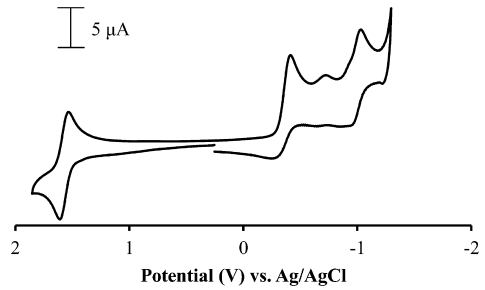

Figure 2. Cyclic voltammogram of **1** measured at RT under Ar in 0.1 M Bu_4NPF_6 in CH_3CN performed at 100 mV s^{-1} using a Pt disc working electrode, Pt wire auxiliary electrode, and Ag wire pseudoreference electrode with ferrocene internal standard and referenced to Ag/AgCl.

Table 1 lists electrochemical data for bimetallic complexes **1** and **2** and the monometallic synthon **1b**.

Table 1. Summary of Electrochemical Data

complex[a]	$E_{1/2}$ (V)	assignment
1	+1.59[d]	$Ru^{II/III}$
	−0.38[e]	$Rh^{III/II}Br_2$, $Rh^{II/I}Br$
	−0.73[f]	$Rh^{II/I}Br_2$
	−0.98	$dpp^{0/-}$
2[b]	+1.59[d]	$Ru^{II/III}$
	−0.37[e]	$Rh^{III/II}Cl_2$, $Rh^{II/I}Cl$
	−0.77[f]	$Rh^{II/I}Cl_2$
	−0.96	$dpp^{0/-}$
1b[c]	+1.40[d]	$Ru^{II/III}$
	−1.02	$dpp^{0/-}$
	−1.37	$Ph_2phen^{0/-}$
	−1.56	$Ph_2phen^{0/-}$

[a]Measured at RT under Ar in 0.1 M Bu_4NPF_6 in CH_3CN performed at 100 mV s^{-1} using a Pt disc working electrode, Pt wire auxiliary electrode, and Ag wire pseudoreference electrode with ferrocene internal standard and referenced to Ag/AgCl. [b]Reference 30. [c]Reference 33. [d]$E_{1/2} = E°$ for reversible process. [e]$E_{1/2}$ of quasi-reversible process. [f]E_p^c of irreversible process.

Anodically, a reversible, one-electron couple ($E_{1/2}$ = +1.59 V vs Ag/AgCl) is assigned as $Ru^{II/III}$. Coordination of the electropositive Rh(III) subunit to **1b** perturbs the electrochemical properties, evidenced with a more positive potential for the $Ru^{II/III}$ couple in the bimetallic complex resulting from Ru(dπ) orbital stabilization to make oxidation of the system more difficult.[33]

Cathodically, electrochemical assignment is complicated by the nearly isoenergetic Rh(dσ*)- and dpp(π*)-based molecular orbitals. The electrochemical mechanism for complex **1** is best described using multiple pathways and is explained in detail in a separate recent publication by our group.[30] The first cathodic wave (E_p^c = −0.38 V) is assigned as overlapping $Rh^{III/II}Br_2$ and $Rh^{II/I}Br$ reductions. The second cathodic wave (E_p^c = −0.73 V) is assigned as $Rh^{II/I}Br_2$ and exists for the fraction of complex that does not undergo halide loss prior to the second Rh-based reduction. A third, quasi-reversible reduction ($E_{1/2}$ = −0.98 V) is assigned as $dpp^{0/-}$ and provides evidence for higher lying BL-based orbitals relative to Rh-based orbitals. A similar electrochemical mechanism exists for the Cl^- bimetallic analogue **2** with the rate of halide loss modulating cathodic differences due to the increased σ-donating ability of Cl^- vs Br^-.[30] Ph_2phen terminal ligand and second dpp reductions are overlapping and occur beyond the first dpp reduction. Cyclic voltammetry establishes a Ru-based HOMO (highest occupied molecular orbital) and Rh-based LUMO for both bimetallic systems, important features for photoinitiated electron collection at Rh.

Electronic Absorption Spectroscopy. Complex **1** is an efficient light absorber in the UV and visible regions of the electromagnetic spectrum. Figure 3 shows the electronic

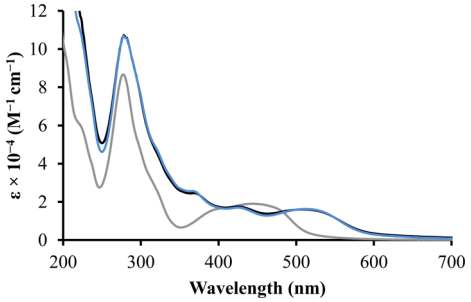

Figure 3. Electronic absorption spectra of **1** (black line), **2** (blue line), and **1b** (gray line), displaying the difference in light absorption upon coordination of a $Rh^{III}Br_2(Ph_2phen)$ moiety. Spectra were obtained in RT CH_3CN in a 1 cm quartz cuvette.

absorption spectra of the new Ru(II),Rh(III) bimetallic complex **1** overlaid with **2** and the monometallic precursor **1b** to illustrate the influence halide variation at Rh as well as coordination of an electropositive metal to the Ru(II) light absorber has on the light-absorbing properties, with tabulated data in Table 2.

The UV is dominated by intraligand (^{1}IL) $\pi \rightarrow \pi^*$ transitions, with λ^{abs} = 278 nm (107 000 M^{-1} cm^{-1}) for Ph_2phen $\pi \rightarrow \pi^*$ transitions and λ^{abs} = 365 nm (24 000 M^{-1} cm^{-1}) for dpp $\pi \rightarrow \pi^*$ transitions. In the visible, singlet metal-to-ligand charge transfer (^{1}MLCT) transitions dominate with Ru(dπ) → $Ph_2phen(\pi^*)$ CT transitions occurring at higher energy (λ^{abs} = 414 nm; 17 000 M^{-1} cm^{-1}) than Ru(dπ) → dpp(π^*) CT transitions (λ^{abs} = 514 nm; 16 000 M^{-1} cm^{-1}).

When compared to precursor **1b**, complex **1** possesses a red-shifted Ru(dπ) → dpp(π^*) CT transition due to stabilization of the dpp(π^*)-based molecular orbitals upon coordination to a second electropositive metal center.[33] The energy of Ph_2phen IL transitions is unaffected by coordination of the Rh(III) subunit; however, the extinction coefficient increases due to an additional chromophoric Ph_2phen ligand. Complex **1** displays nearly identical light-absorbing properties to **2**.[29] This trend is

DOI: 10.1021/acs.inorgchem.5b00116
Inorg. Chem. 2015, 54, 3545−3551

Table 2. Summary of Light-Absorbing Properties

complex[a]	λ^{abs} (nm)	$\varepsilon \times 10^{-4}$ (M^{-1} cm^{-1})	assignment
1	278	10.7	Ph_2phen $\pi \rightarrow \pi^*$
	365	2.4	dpp $\pi \rightarrow \pi^*$
	414	1.7	Ru(dπ) $\rightarrow$ $Ph_2phen(\pi^*)$ CT
	514	1.6	Ru(dπ) $\rightarrow$ dpp(π^*) CT
2[b]	278	10.7	Ph_2phen $\pi \rightarrow \pi^*$
	365	2.6	dpp $\pi \rightarrow \pi^*$
	414	1.7	Ru(dπ) $\rightarrow$ $Ph_2phen(\pi^*)$ CT
	514	1.6	Ru(dπ) $\rightarrow$ dpp(π^*) CT
1b[c]	274	8.4	Ph_2phen $\pi \rightarrow \pi^*$
	309	3.4	dpp $\pi \rightarrow \pi^*$
	424	1.8	Ru(dπ) $\rightarrow$ $Ph_2phen(\pi^*)$ CT
	474	1.7	Ru(dπ) $\rightarrow$ dpp(π^*) CT

[a]Measured at RT in CH_3CN in a 1 cm quartz cuvette. [b]Values consistent with those in ref 29. [c]Values consistent with those in ref 33.

expected because the component varied is a nonchromophoric ligand.

Steady-State and Time-Resolved Emission Spectroscopy. The emissive nature of the lowest lying Ru(dπ) $\rightarrow$ dpp(π^*) ^{3}MLCT excited state of complex **1** provides a probe into the excited-state dynamics of this complex. Variation of the halide coordinated to Rh in complexes **1** and **2** from Br^- to Cl^- does not impact the excited-state properties (Figure 4), tabulated in Table 3 with comparison to the monometallic precursor **1b**.

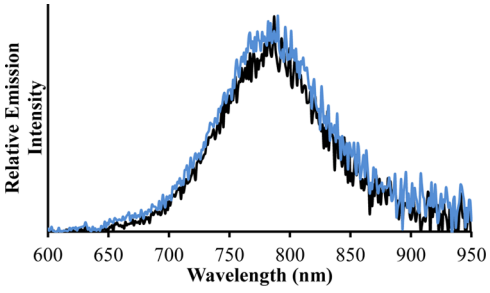

Figure 4. Emission spectra of **1** (black line) and **2** (blue line). Spectra were obtained in RT CH_3CN in a 1 cm quartz cuvette and were corrected for PMT response.

Complexes **1**, **2**, and **1b** undergo excitation to a ^{1}MLCT excited state followed by intersystem crossing to populate a ^{3}MLCT excited state with unity efficiency. Upon coordination of a second electropositive metal in the Ru(II),Rh(III) bimetallic architectures, Rh(dσ^*)-based acceptor orbitals become accessible to facilitate population of a low-energy ^{3}MMCT excited state. Deactivation from the ^{3}MMCT excited state can occur through nonradiative decay (k_{nr}') back to the ^{1}GS or through a photochemical reaction (k_{rxn}) (Figure 5).

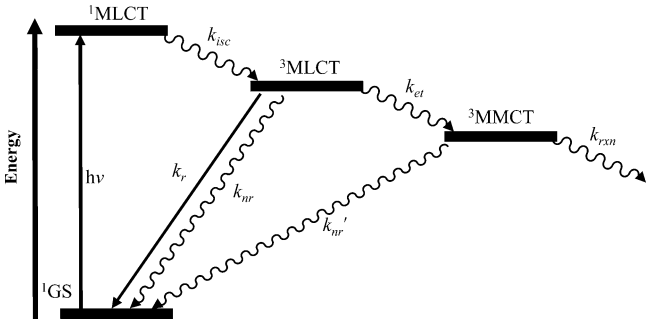

Figure 5. Simplified Jablonski-type state diagram for **1** and **2**. ^{1}GS = singlet ground state; k_{isc} = rate of intersystem crossing; k_r = rate of radiative decay; k_{nr} = rate of nonradiative decay; k_{et} = rate of intramolecular electron transfer; k_{rxn} = rate of photochemical reaction.

Variation of the halide coordinated to Rh in complexes **1** and **2** from Br^- to Cl^- produces identical steady-state and time-resolved emission properties in RT acetonitrile (λ^{em} = 780 nm, $\Phi^{em} = 1.3 \times 10^{-4}$, τ = 46 ns, $k_r = 2.8 \times 10^3$ s^{-1}, $k_{nr} = 5.2 \times 10^6$ s^{-1}), indicating equivalent rates of population of the low-lying ^{3}MMCT excited state ($k_{et} = 1.6 \times 10^7$ s^{-1}) when the halide coordinated to Rh is Br^- or Cl^-. Compared to the bimetallic model complex $[\{(Ph_2phen)_2Ru\}_2(dpp)]^{4+}$ that lacks a ^{3}MMCT excited state,[27] complexes **1** and **2** display quenched emission of the ^{3}MLCT excited state to validate ^{3}MMCT excited-state population required for photocatalysis. At 77 K in a rigid glass matrix, intramolecular electron transfer is impeded, providing further validation for RT ^{3}MLCT excited-state quenching in these Ru(II),Rh(III) bimetallic systems.

In analogous motifs, quantum yield and excited-state lifetime values are influenced by halide identity.[25−27] Smaller Φ^{em} and shorter τ in such systems with Br^- ligands coordiated to Rh suggest more efficient population of a low-lying ^{3}MMCT excited state (faster k_{et}) that contributes to enhanced photocatalytic activity in the Br^- trimetallic system. Despite identical excited-state properties and k_{et} values for the Br^- and Cl^- bimetallic supramolecules, complex **1** is still photocatalytically superior. Thus, complexes **1** and **2** provide an ideal forum to study the impact of halide identity on photocatalytic H_2 generation when excited-state properties are identical.

Photocatalytic H_2 Production. H_2 production experiments were carried out to determine the role of halide variation in the Ru(II),Rh(III) supramolecular photocatalyst system. The Cl^- bimetallic analogue **2** is a photocatalyst for H_2O reduction.[29] The bimetallic complex undergoes light-assisted collection of reducing equivalents at Rh to produce an intact Ru(II),Rh(I) species that is the proposed active photocatalyst. With the substitution of Br^- for Cl^- halides shown herein to not greatly perturb spectroscopic and electrochemical properties, it is not surprising that **1** also serves as a photocatalyst for H_2 production (Figure 6A).

Table 3. Summary of Photophysical Data

	RT[a]						77 K[b]	
complex	λ^{em} (nm)	Φ^{em} (10^{-4})	τ (ns)	k_r (10^3 s^{-1})	k_{nr} (10^6 s^{-1})	k_{et} (10^7 s^{-1})	λ^{em} (nm)	τ (μs)
1	780	1.3	46	2.8	5.2	1.6	706	1.6
2	780	1.3	46	2.8	5.2	1.6	706	1.8
1b[c]	664	350	820	43	1.2		607	5.4

[a]Measured at RT in CH_3CN deoxygenated with Ar in a 1 cm quartz cuvette. [b]Measured in 4:1 ethanol/methanol at 77 K. [c]Reference 33.

DOI: 10.1021/acs.inorgchem.5b00116
Inorg. Chem. 2015, 54, 3545−3551

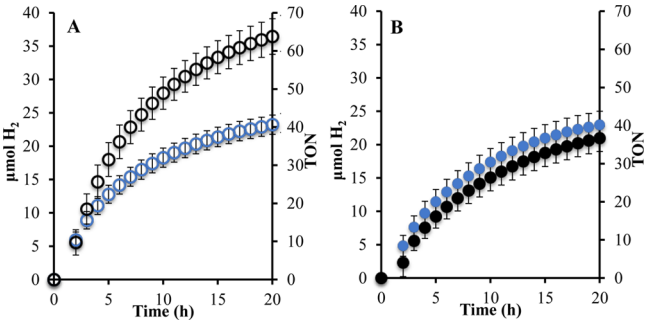

Figure 6. Hydrogen production profiles for **1** and **2** in Ar-deoxygenated DMF solvent. (A) (Black open circles) **1**; (blue open circles) **2**. (B) (Black filled circles) **1** with 260 μM Bu_4NCl; (blue filled circles) **2** with 260 μM Bu_4NBr. Systems contained 130 μM photocatalyst, 0.62 M H_2O, 1.5 M DMA electron donor, and 110 μM $[DMAH^+][CF_3SO_3^-]$.

When photolyzed for 20 h with λ = 470 nm light in DMF (*N*,*N*-dimethylformamide) solvent in the presence of H_2O and DMA (*N*,*N*-dimethylaniline) electron donor, complex **1** produces 36 ± 3 μmol of H_2 (62 ± 5 TON = turnover number = mol H_2 produced/mol catalyst), an increase in H_2 production compared to **2**, 23 ± 1 μmol of H_2 (40 ± 2 TON). DMF was chosen as the solvent for these photocatalytic studies because its weaker ligating ability leads to enhanced photocatalysis.[29] The improved photocatalytic ability of **1** relative to **2** is a unique result considering that the two complexes have identical excited-state properties (Φ^{em} and τ), values that are different in analogous Ru(II),Rh(III),Ru(II) trimetallic supramolecules.[25−27] Therefore, the discrepancy in H_2 production between the Ru(II),Rh(III) bimetallic systems described herein cannot be ascribed to differences in excited-state properties.

With knowledge that H_2 production is impacted by halide variation in Ru(II),Rh(III) bimetallic supramolecules possessing identical light-absorbing and excited-state properties, the influence of halide was further investigated. Upon reduction of Rh by two equivalents, two halide ligands are lost to produce the square planar Rh(I)-containing supramolecule, yet these halides still seem to play an important role in photocatalysis. The close proximity of the halide ion to the metal complex, made possible by ion pairing in low-dielectric solvents such as DMF, may alter catalyst function by providing a high local concentration of halide ion to hinder interaction of the Rh(I) center with H_2O due to halide recoordination.

Interestingly, when H_2 experiments were carried out adding two equivalents (260 μM) of the opposite halide to the photolysis solutions for each photocatalyst, accounting for two equivalents of halide lost, both systems demonstrated identical photocatalytic activity (Figure 6B). Using photocatalyst **1**, 260 μM Bu_4NCl (tetra-*n*-butylammonium chloride) was added to the photolysis solution, producing 21 ± 2 μmol of H_2 (36 ± 3 TON) after 20 h photolysis. Conversely, 260 μM Bu_4NBr (tetra-*n*-butylammonium bromide) was added to the photolysis solution utilizing photocatalyst **2** and produced 23 ± 2 μmol of H_2 (39 ± 4 TON) after 20 h. These experimental conditions allow for equal concentrations of Br^- and Cl^- in solution following generation of the active Ru(II),Rh(I) catalyst.

Complex **1** showed a decrease of 20 TONs with added Cl^- relative to the H_2 experiment with no added halide, while complex **2** only showed a decrease of ∼1 TON upon added Br^-. A local high concentration of halide ion promotes halide recoordination to the catalytically active Rh(I), impeding its interactions with H_2O and affording lower H_2 yields. Recoordination of the halide via formation of an ion-paired complex between the halide and the photocatalyst is probable and has been shown as a deactivation pathway for other homogeneous transition metal catalysts.[41] The added Cl^- more negatively affects catalysis relative to added Br^-, demonstrating that the more σ-donating Cl^- ligands can ion pair more strongly with the photocatalyst and inhibit catalyst function. By contrast, bulkier and less strongly σ-donating Br^- addition does not impact catalysis as significantly, consistent with a comparatively weaker ion pair formed between Br^- and the photocatalyst and supporting increased H_2 production in Br^- analogues of Ru(II),Rh(III) photocatalysts.

CONCLUSION

The new complex **1** was synthesized and characterized to explore the impact of halide variation on spectroscopic and electrochemical properties as well as on photocatalytic H_2 production capabilities relative to the previously reported Cl^- bimetallic supramolecule. Cyclic voltammetry of complex **1** provides evidence for a Ru-based HOMO and a Rh-based LUMO which are requirements for H_2O reduction photocatalysis via photoinitiated electron collection at Rh. The complex absorbs light in the UV with ligand $\pi \rightarrow \pi^*$ transitions and in the visible with Ru(dπ) → ligand(π^*) ^{1}MLCT transitions (ligand = Ph_2phen or dpp). Radiative decay from a ^{3}MLCT excited state shows a relatively low quantum yield of emission and short excited-state lifetime due to population of a low-energy ^{3}MMCT excited state, necessary behavior for electron collection at the Rh site to achieve active H_2 photocatalysts. With light absorption in the visible and collection of reducing equivalents on a Rh-based LUMO, complex **1** is a photocatalyst for H_2O reduction and displays enhanced activity compared to the Cl^- analogue **2**. Added halide experiments indicate that ion pairing deactivates the catalyst due to the local concentration of halide ion in proximity to the photocatalyst, with the more σ-donating Cl^- ligands more negatively influencing photocatalysis relative to Br^-. These results are significant because they provide remarkable evidence showing that halide identity impacts catalysis even after halides are dissociated to form the Rh(I)-containing photocatalyst. Studies are ongoing in our laboratory to examine potential catalytic intermediates that involve ligand variation at the Rh center as the complex cycles from Rh(III) to Rh(I) to produce H_2 from H_2O.

AUTHOR INFORMATION

Corresponding Author

*E-mail: hannahm@vt.edu.

Notes

The authors declare no competing financial interest.

†Karen J. Brewer is deceased.

ACKNOWLEDGMENTS

Acknowledgement is made to the Chemical Sciences, Geosciences and Biosciences Division, Office of Basic Energy Sciences, Office of Sciences, U.S. Department of Energy (DE FG02-05ER15751), for their generous financial support of the work described herein. Special thanks are given to Dr. James Tanko and Ms. Kristen Felice for assistance with this manuscript. Mr. William Bebout of the Virginia Tech

DOI: 10.1021/acs.inorgchem.5b00116
Inorg. Chem. 2015, 54, 3545−3551

Department of Chemistry Analytical Services Laboratory is acknowledged for assistance with mass spectral data.

REFERENCES

(1) Bard, A. J.; Fox, M. A. *Acc. Chem. Res.* **1995**, *28*, 141−145.
(2) Lewis, N. S.; Nocera, D. G. *Proc. Natl. Acad. Sci. U.S.A.* **2006**, *103*, 15729−15735.
(3) Kirch, M.; Lehn, J. M.; Sauvage, J. P. *Helv. Chim. Acta* **1979**, *62*, 1345−1384.
(4) Balzani, V.; Bergamini, G.; Campagna, S.; Puntoriero, F. In *Photochemistry and Photophysics of Coordination Compounds I*; Balzani, V., Campagna, S., Eds.; Springer-Verlag Berlin: Berlin, 2007; Vol. *280*, pp 1−36.
(5) Denti, G.; Campagna, S.; Sabatino, L.; Serrni, S.; Ciano, M.; Balzani, V. *Inorg. Chem.* **1990**, *29*, 4750−4758.
(6) Balzani, V.; Moggi, L.; Scandola, F. In *Supramolecular Photochemistry*; Balzani, V., Ed.; NATO ASI Series 214; Reidel: Dordrecht, The Netherlands, 1987; pp 1−28.
(7) Holliday, B. J.; Mirkin, C. A. *Angew. Chem., Int. Ed.* **2001**, *40*, 2022−2043.
(8) Kalyanasundaram, K.; Gratzel, M.; Nazeeruddin, M. K. *J. Phys. Chem.* **1992**, *96*, 5865−5872.
(9) Kalyanasundaram, K. *Photochemistry of Polypyridine and Porphyrin Complexes*; Academic Press: London, 1992.
(10) Kalyanasundaram, K. *Coord. Chem. Rev.* **1982**, *46*, 159−244.
(11) Vanhouten, J.; Watts, R. J. *J. Am. Chem. Soc.* **1976**, *98*, 4853−4858.
(12) Vanhouten, J.; Watts, R. J. *Inorg. Chem.* **1978**, *17*, 3381−3385.
(13) Meyer, T. J. *Pure Appl. Chem.* **1986**, *58*, 1193−1206.
(14) Brewer, K. J.; Murphy, W. R.; Spurlin, S. R.; Petersen, J. D. *Inorg. Chem.* **1986**, *25*, 882−884.
(15) Wallace, A. W.; Murphy, W. R.; Petersen, J. D. *Inorg. Chim. Acta* **1989**, *166*, 47−54.
(16) Schulz, M.; Karnahl, M.; Schwalbe, M.; Vos, J. G. *Coord. Chem. Rev.* **2012**, *256*, 1682−1705.
(17) Mongelli, M. T.; Brewer, K. J. *Inorg. Chem. Commun.* **2006**, *9*, 877−881.
(18) Zigler, D. F.; Wang, J.; Brewer, K. J. *Inorg. Chem.* **2008**, *47*, 11342−11350.
(19) Konduri, R.; Ye, H. W.; MacDonnell, F. M.; Serroni, S.; Campagna, S.; Rajeshwar, K. *Angew. Chem., Int. Ed.* **2002**, *41*, 3185−3187.
(20) Molnar, S. M.; Nallas, G.; Bridgewater, J. S.; Brewer, K. J. *J. Am. Chem. Soc.* **1994**, *116*, 5206−5210.
(21) Fukushima, T.; Fujita, E.; Muckerman, J. T.; Polyansky, D. E.; Wada, T.; Tanaka, K. *Inorg. Chem.* **2009**, *48*, 11510−11512.
(22) Polyansky, D. E.; Cabelli, D.; Muckerman, J. T.; Fukushima, T.; Tanaka, K.; Fujita, E. *Inorg. Chem.* **2008**, *47*, 3958−3968.
(23) Polyansky, D.; Cabelli, D.; Muckerman, J. T.; Fujita, E.; Koizumi, T.; Fukushima, T.; Wada, T.; Tanaka, K. *Angew. Chem., Int. Ed.* **2007**, *46*, 4169−4172.
(24) Elvington, M.; Brown, J.; Arachchige, S. M.; Brewer, K. J. *J. Am. Chem. Soc.* **2007**, *129*, 10644−10645.
(25) Arachchige, S. M.; Brown, J.; Brewer, K. J. *J. Photochem. Photobiol. A: Chem.* **2008**, *197*, 13−17.
(26) White, T. A.; Rangan, K.; Brewer, K. J. *J. Photochem. Photobiol. A: Chem.* **2010**, *209*, 203−209.
(27) White, T. A.; Higgins, S. L. H.; Arachchige, S. M.; Brewer, K. J. *Angew. Chem., Int. Ed.* **2011**, *50*, 12209−12213.
(28) Wang, J.; White, T. A.; Arachchige, S. M.; Brewer, K. J. *Chem. Commun.* **2011**, *47*, 4451−4453.
(29) White, T. A.; Whitaker, B. N.; Brewer, K. J. *J. Am. Chem. Soc.* **2011**, *133*, 15332−15334.
(30) White, T. A.; Mallalieu, H. E.; Wang, J.; Brewer, K. J. *Chem.—Eur. J.* **2014**, *20*, 8265−8268.
(31) Zhou, R.; Sedai, B.; Manbeck, G. F.; Brewer, K. J. *Inorg. Chem.* **2013**, *52*, 13314−13324.
(32) Basile, L. A.; Barton, J. K. *J. Am. Chem. Soc.* **1987**, *109*, 7548−7550.
(33) Higgins, S. L. H.; White, T. A.; Winkel, B. S. J.; Brewer, K. J. *Inorg. Chem.* **2011**, *50*, 463−470.
(34) Sau, Y.-K.; Chan, K.-W.; Zhang, Q.-F.; Williams, I. D.; Leung, W.-H. *Organometallics* **2007**, *26*, 6338−6345.
(35) Gennett, T.; Milner, D. F.; Weaver, M. J. *J. Phys. Chem.* **1985**, *89*, 2787−2794.
(36) Caspar, J. V.; Kober, E. M.; Sullivan, B. P.; Meyer, T. J. *J. Am. Chem. Soc.* **1982**, *104*, 630−632.
(37) Brown, J. R.; Elvington, M.; Mongelli, M. T.; Zigler, D. F.; Brewer, K. J. *Proc. SPIE* **2006**, *6340*, 634017-1 −634017-10.
(38) Rasmussen, S. C.; Richter, M. M.; Yi, E.; Place, H.; Brewer, K. J. *Inorg. Chem.* **1990**, *29*, 3926−3932.
(39) Bolinger, C. M.; Story, N.; Sullivan, B. P.; Meyer, T. J. *Inorg. Chem.* **1988**, *27*, 4582−4587.
(40) Kew, G.; DeArmond, K.; Hanck, K. *J. Phys. Chem.* **1974**, *78*, 727−734.
(41) Crabtree, R. H. *Chem. Rev.* **2015**, *115*, 127−150.

DOI: 10.1021/acs.inorgchem.5b00116
Inorg. Chem. 2015, 54, 3545−3551